International Journal of Applied Science and Engineering
2009. 7, 2: 95-114

Double Friction Dampers for Wind Excited Benchmark Building

V. B. Patil* and R. S. Jangid

Department of Civil Engineering,
Indian Institute of Technology Bombay, Powai, Mumbai – 400 076, India

Abstract: A modified friction damper is presented to enhance the performance of conventional friction damper and semi-active variable friction damper. An additional plate is provided between the two sliding plates of a conventional friction damper which results in an additional sliding interface with the same normal (clamping) force. Similar modification is also made to semi-active variable friction damper (SAVFD) to enhance its performance. The enhancement in the performance of the benchmark building is studied under across wind loads by installing the modified dampers. The governing equations of motion are solved by employing state space theory. Optimization of location and number of dampers is also carried out with the help of a controllability index which is obtained with the help of root-mean-square (RMS) value of the inter-storey drift. Further, a parametric study of passive friction dampers by varying slip force is carried out. From the numerical study, it is found that both double friction damper and semi-active variable double friction damper (SAVDFD) are quite effective in enhancing the performance of the benchmark building. At optimized locations, both the proposed dampers give significant enhancement in the performance of the benchmark building.

Keywords: Tall building; passive damper; semi-active control; double friction; wind load

1. Introduction

Various structural control methods like passive control, active control, semi-active control and hybrid control have been studied on different buildings for different dynamic loads. Significant progress has also been made in the area of structural control. Some of the control methods have been implemented for real structures. However, to streamline and focus the study of structural control on the same building with the same load, the concept of benchmark problems has come into picture. Therefore, based on realistic full scale buildings, two structural control benchmark problems have been proposed for earthquake and wind excitations [1]. The wind excited benchmark building is a 76-storey, 306 m concrete office tower proposed for the city of Melbourne, Australia. The building is tall and slender with a height to width ratio of 7.3; hence it is wind sensitive. Wind tunnel tests [2] for the 76-storey building model have been conducted at the University of Sydney and the results of across-wind data are provided for the analysis of the benchmark problem.

Performance of various dampers like tuned liquid column dampers [3], liquid column vibration absorbers [4], hybrid viscous-tuned liquid column damper [5], variable stiffness

* Corresponding author; e-mail: rsjangid@civil.iitb.ac.in *Accepted for Publication: January 8, 2010,*

tuned mass damper [6] on the benchmark building have been studied. Patil and Jangid (2009) [7] studied the response of the benchmark building with the various arrangements of linear viscous dampers and SAVFDs by connecting them to alternative floors of the building.

A typical friction damper usually consists of a frictional sliding interface and a clamping mechanism that produces normal contact force on the interface. Bhaskararao and Jangid (2006a) proposed two numerical models to evaluate the frictional force in the connected dampers for multi-degree of freedom (MDOF) structures and validated with the results obtained from the analytical model considering an example of single degree of freedom (SDOF) structures [8]. Further, the effectiveness of dampers in terms of the reduction of structural responses, of connected adjacent structures is investigated. They also conducted a parametric study to investigate the optimum slip force of the damper. In addition, the authors studied the optimal placement of dampers. So far the conventional dampers have been used to control the vibration of the structures. Bhaskararao and Jangid (2006b) studied the dynamic response of two adjacent single story building structures connected with a friction damper under harmonic ground excitation [9]. Here, an attempt is made to enhance the performance of friction dampers by providing an additional plate (Figure 1) between the two existing plates and make an additional interface available to resist the external loads.

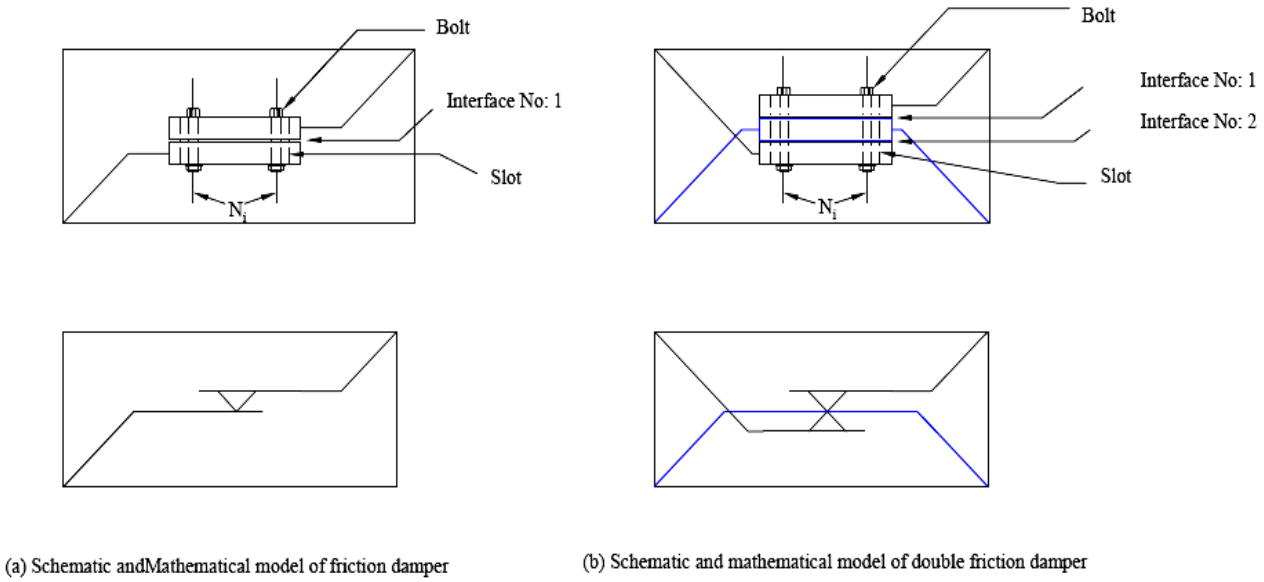

(a) Schematic andMathematical model of friction damper

(b) Schematic and mathematical model of double friction damper

Figure 1. Schematic and mathematical models of conventional and double friction dampers

Further, to improve the performance of passive dampers semi-active dampers are proposed in the literature. A semi-active friction damper is able to adjust its slip force by controlling its clamping force in real-time, depending on the structure's motion during an earthquake. This adaptive nature makes a semi-active friction damper more efficient. The control by semi-active friction dampers requires a feedback control algorithm and on-line measurement of structural response in order to determine the appropriate level of adjustable clamping forces of the dampers. Akbay and Aktan (1995) [10] proposed the control algorithm that determines the clamping force at the next time step. Other proposed

control laws include the bang-bang control [11], modulated homogenous control (Inaudi, 1997) [12], linear quadratic regulator [13], friction-force incremental control [14], modal control (Lu and Chung, 2001; Lu, 2004a) [15,16], predictive control [17], modal and optimal control [18].

Kori and Jangid (2008) [19] studied the performance of SAVFDs by placing them at various floors of multi-storey buildings using predictive control law. Predictive control algorithm is able to keep the friction force of a semi-active friction damper slightly lower than the critical friction force, so that the damper is kept continuously slipping to avoid the unwanted high frequency structural response which would have been produced in passive friction dampers. This results in better energy dissipation. The method is formulated in a discrete-time domain and cast in the form of direct output feedback for easy control implementation. Thus investigation on predictive control algorithm method was focused on predicting the critical friction force, but with a single sliding surface for each damper.

By providing an additional friction pad (Figure 2) on the inner side of the clamping mechanism of a SAVFD an additional resisting interface is brought into use with the same clamping mechanism, thus enhancing the resisting frictional force. This is how a SAVFD is converted into a semi-active double friction damper (SAVDFD). This SAVDFD is used to study the performance of wind excited benchmark building.

Optimization of location and number of dampers is also carried out by adopting a sequential search procedure [20] with the help of a controllability index which is obtained with the help of RMS value of inter-storey drift.

Thus, the need of the present study is to evaluate the enhancement in the performance of double friction dampers and SAVDFDs as compared to their conventional counterparts on the wind excited benchmark building subjected to across wind loads. The specific objectives of the present study may be summarized as:(i) to study the improvement in the performance of wind excited benchmark building with the proposed double friction dampers and SAVDFDs, as compared to their conventional counterparts installed in all the floors, (ii) to study the reduction in the number of double friction dampers compared to conventional friction dampers both at their optimized locations, to achieve the performance criteria comparable to those obtained with the conventional friction dampers installed in all the floors, (iii) to study the reduction in the number of SAVDFDs as compared to SAVFDs both at their optimized locations, to achieve the performance criteria comparable to those obtained with the SAVFDs installed in all the floors and (iv) to optimize the slip force of conventional friction dampers and double friction dampers at their optimized location and numbers.

2. Benchmark Building

The wind excited benchmark building is a 76-storey 306 m office tower proposed for the city of Melbourne, Australia. The plan and elevation are shown in Figure 3. The building is a reinforced cement concrete building consisting of a concrete core and concrete frame. The mass density of the building is 300 kg per cubic meter. The building is slender with a height-to-width ratio of 306.1/42=7.288; therefore, it is wind sensitive.

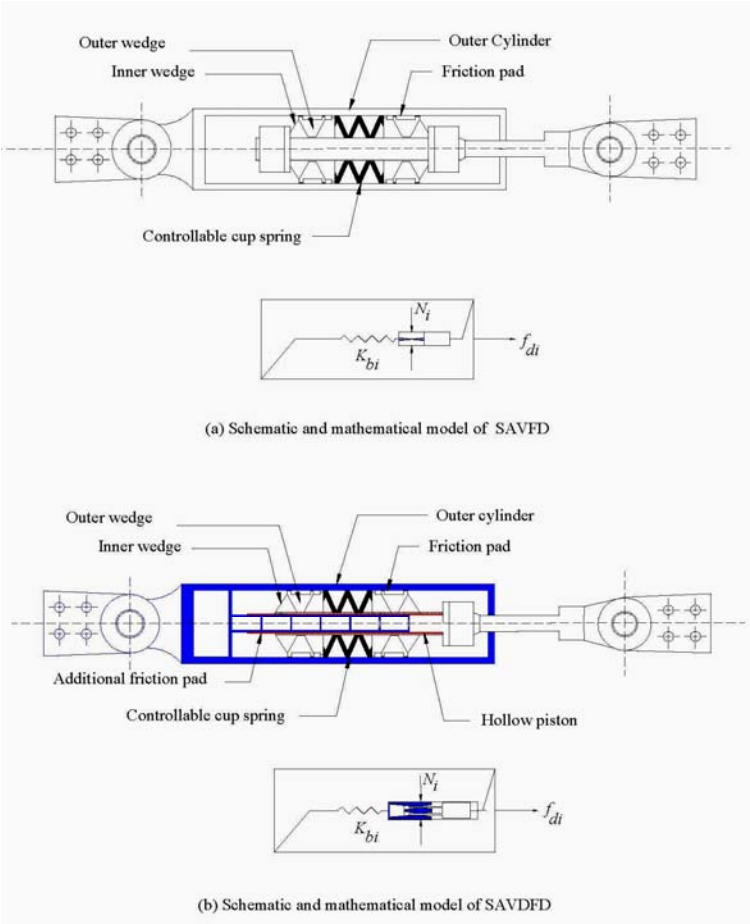

Figure 2. Schematic and mathematical models of SAVFD and SAVDFD (Modified after Kori and Jangid,2008)

The outer dimension for the central reinforced concrete core is 21m×21m. The 24 columns on the periphery of the building are distributed equally on each of the four sides of the building. These columns are connected to a 900 mm deep and 400 mm wide beam on each floor. The lightweight floor construction is made up of steel beams with a metal deck and a 120 mm slab. The compressive strength of concrete is 60 MPa and the modulus of elasticity is 40 GPa. Column sizes, core wall thickness, and floor mass are varying along the height. The building has six plant rooms. The building is modeled as a vertical cantilever beam (Bernoulli–Euler beam). The portion of the building between adjacent floors is considered as a classical beam and the finite element model (FEM) is constructed. The 76 rotational degrees of freedom have been removed by the static condensation. This results in 76 degrees of freedom, representing the displacement of each floor in the lateral direction. The mass matrix **M** and stiffness matrix **K** each of order (76×76) are constructed for the FEM model of the building and provided for the analysis. The first five natural frequencies of the model are 0.16, 0.765, 1.992, 3.790, and 6.395 Hz. $\zeta = 1\%$ is assumed for the first five modes to construct the damping matrix **C** of order (76×76) using Rayleigh's approach [1].

The performance criteria (J_1-J_{12}) defined for the building is given in Table 1.

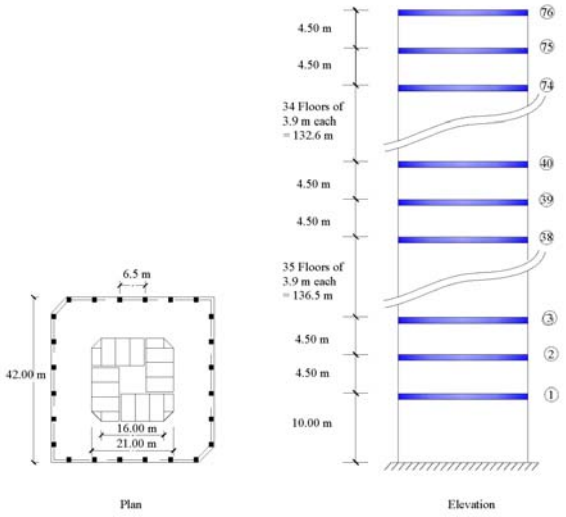

Figure 3. Benchmark Building [1]

Table 1. Performance criteria of the benchmark building

Performance Criteria	Expression
J_1	$\max(\sigma_{\ddot{x}1}, \sigma_{\ddot{x}30}, \sigma_{\ddot{x}50}, \sigma_{\ddot{x}55}, \sigma_{\ddot{x}60}, \sigma_{\ddot{x}65}, \sigma_{\ddot{x}70}, \sigma_{\ddot{x}75}) / \sigma_{\ddot{x}75o}$
J_2	$\frac{1}{6}\sum_i (\sigma_{\ddot{x}i} / \sigma_{\ddot{x}io})$; for i =50, 55, 60, 65, 70, and 75
J_3	$\sigma_{x76} / \sigma_{x76o}$
J_4	$\frac{1}{7}\sum_i \sigma_{xi} / \sigma_{xio}$; for i=50,55,60,65,70,75 and 76
J_5	$\sigma_{xm} / \sigma_{x76o}$
J_6	$\sigma_p = \sqrt{\left\{\frac{1}{T}\int_0^T \left[\dot{x}_m(t)u(t)\right]^2 dt\right\}}$
J_7	$\max(\ddot{x}_{p1}, \ddot{x}_{p30}, \ddot{x}_{p50}, \ddot{x}_{p55}, \ddot{x}_{p60}, \ddot{x}_{p65}, \ddot{x}_{p70}, \ddot{x}_{p75}) / \ddot{x}_{p75o}$
J_8	$\frac{1}{6}\sum_i \ddot{x}_{pi} / \ddot{x}_{pio}$; for i = 50, 55, 60, 65, 70, and 75
J_9	x_{p76} / x_{p76o}
J_{10}	$\frac{1}{7}\sum_i x_{pi} / x_{pio}$; for i = 50, 55, 60, 65, 70, 75, and 76
J_{11}	x_{pm} / x_{p76o}
J_{12}	$P_{\max} = \max\left\|\dot{x}_m(t)u(t)\right\|$

2.1 Friction Damper

Friction dampers are usually classified as one of the displacement-dependant energy dissipation devices and the damper force is independent of the velocity and frequency content of excitation [16]. The friction dampers have advantages such as simple mechanism, low cost, less maintenance and powerful energy dissipation capability as compared to other passive dampers. They were found to be very effective for the seismic design of structures as well as the rehabilitation and strengthening of existing structures They provide a practical, economical and effective approach for the design of structures to resist excessive vibrations. Modeling of frictional force is done using hysteretic model which is a continuous model of the frictional force proposed by Constantinou *et al,* 1990. [21] The frictional forces developed in the dampers are expressed by

$$f_{di} = f_{si} Z_i \text{ for} \left(i=1-r\right) \tag{1}$$

where, Z_i is a non-dimensional hysteretic component satisfying the following non-linear first order differential equation, which is expressed as

$$q\frac{\mathrm{d}Z_i}{\mathrm{d}t} = A(\dot{x}_{i2} - \dot{x}_{i1}) - \beta\left|(\dot{x}_{i2} - \dot{x}_{i1})\right| Z_i \left|Z_i\right|^{n-1} - \tau(\dot{x}_{i2} - \dot{x}_{i1})\left|Z_i\right|^n \tag{1.a}$$

where, q is the yield displacement; β, τ, n and A are non-dimensional parameters of the hysteretic loop. The parameters β, τ, n and A control the shape of the loop and are selected such as to provide a rigid-plastic behavior (typical Coulomb-friction behavior). The recommended values for the above parameters are: q = 0.1 mm, A = 1, β = 0.5, τ = 0.5 and n = 2. The hysteretic displacement component, Z_i is bounded by its peak values of ±1 to account for the conditions of sliding and non-sliding phases.

And for a SAVDFD, as the number of interfaces is 2, the frictional forces developed in the dampers are modified as

$$f_{di} = 2 f_{si} Z_i \text{ for} \left(i=1-r\right) \tag{1.b}$$

2.2 Semi-Active Variable Double Friction Damper

In order to improve the performance of friction dampers, the concept of semi-active control is introduced to the dampers. A semi-active friction damper is able to adjust its slip force by controlling its clamping force in real-time in response to a structure's motion during a wind. Because of this adaptive nature, a semi-active friction damper is expected to be more effective than a passive damper. On the other hand, just like in active structural control, the control of semi-active friction dampers requires a feedback control algorithm and online measurement of structural response in order to determine the appropriate level of adjustable clamping forces of the dampers. Nevertheless, a semi-active control device generally has the following advantages over an active control one (i) because the control action is carried out by adjusting the internal mechanism (i.e., the clamping force for a semi-active friction damper), the required control stroke and energy can be very small; and (ii) because it does not pump energy into the controlled structures, control instability can be prevented. As already mentioned, the control of semi-active dampers requires a control algorithm. Needless to say, the control performance of the semi-active dampers significantly relies on the control algorithm applied. One of the recent control laws "predictive control

law" [17] which determines the vector of critical friction forces for the next time step is given by;

$$\tilde{\mathbf{u}}[k] = \mathbf{G}_z\mathbf{z}[k-1] + \mathbf{G}_u\mathbf{u}[k-1] + \mathbf{G}_w\mathbf{F}[k-1] \quad (2)$$

The physical meaning of the i^{th} element $\tilde{u}_i[\mathrm{k}]$ in the vector $\tilde{\mathbf{u}}[\mathrm{k}]$ is the minimum friction force required by the i^{th} damper at k^{th} time step, in order to keep the damper in its stick state (or prevent the damper from entering the slip state). By applying a normal force $N_i[k]$ for i^{th} damper such that the resulting slip force is slightly less than the value $\tilde{u}_i[k]$ predicted by equation (2) the damper can be brought into slip state.

$$N_i[k] = \mathrm{R}_f \frac{|\tilde{u}_i[k]|}{\mu} \quad 0 \le \mathrm{R}_f < 1 \ (\text{for } i = 1\text{-}r) \quad (2.a)$$

Thus, the control force vector when all the dampers are brought into slip state is given by,

$$\mathbf{u}[k] = \mathrm{R}_f\tilde{\mathbf{u}}[k] \quad (2.b)$$

where, R_f *is* a gain multiplier defined as the ratio of damper force to critical damper control force and plays an important role in the present control law.

where,

$$\mathbf{G}_z = \mathbf{K}_\mathrm{b}\mathbf{D}(\mathbf{A}_\mathrm{d} - \mathbf{I}) \quad (2.c)$$

$$\mathbf{G}_u = \mathbf{K}_\mathrm{b}\mathbf{D}\mathbf{B}_\mathrm{d} + \mathbf{I} \quad (2.d)$$

$$\mathbf{G}_w = \mathbf{K}_\mathrm{b}\mathbf{D}\mathbf{E}_\mathrm{d} \quad (2.e)$$

After being multiplied by the factor R_f, these matrices may also be treated as the control gains. where,

$$\mathbf{B}_\mathrm{d} = \mathbf{A}^{-1}(\mathbf{A}_\mathrm{d} - \mathbf{I})\mathbf{B} \quad (2.f)$$

$$\mathbf{E}_\mathrm{d} = \mathbf{A}^{-1}(\mathbf{A}_\mathrm{d} - \mathbf{I})\mathbf{E} \quad (2.g)$$

where,

$$\mathbf{B} = \begin{bmatrix} \mathbf{0} \\ \mathbf{M}^{-1}\mathbf{\Lambda} \end{bmatrix}; \quad \mathbf{E} = \begin{bmatrix} \mathbf{0} \\ \mathbf{M}^{-1} \end{bmatrix} \quad (2.h)$$

Let **y** be a vector listing all damper elongations (deformations) that are equal to the drifts of the stories on which the dampers are installed. At any given instant in time, the relation between y and the state of the structure **z** may be written as

$$\mathbf{y}[k] = \mathbf{D}\mathbf{z}[k] \quad (2.i)$$

For a SAVDFD, the number of interface available is 2; the control force offered by i^{th} device is given by,

$$\mathrm{u}_i[k] = 2\mathrm{R}_f\tilde{\mathrm{u}}_i[k] \quad (2.j)$$

2.3 Governing Equations of Motion

The governing equation of motion for the controlled building structure model subjected to wind excitations can be written as

$$\mathbf{M}\ddot{\mathbf{x}} + \mathbf{C}\dot{\mathbf{x}} + \mathbf{K}\mathbf{x} + \mathbf{\Lambda}\mathbf{u} = \mathbf{F} \quad (3)$$

where **x** is displacement vector, $\dot{\mathbf{x}}$ and $\ddot{\mathbf{x}}$ the first and second time derivatives, **M**, **C** and **K** are mass, damping and stiffness matrices respectively; $\mathbf{u}=[f_{d1}, f_{d2}, \ldots f_{dr}]^\mathrm{T}$ and **F** are control force vector and wind load vector respectively; **Λ** is a matrix of zeros and ones, where 1 will indicate where the damper force is being applied.

$$\dot{\mathbf{z}} = \mathbf{A}\mathbf{z} + \mathbf{B}\mathbf{u} + \mathbf{E}\mathbf{F} \quad (4)$$

where **z** is the state vector of structure, and contains displacement and velocity of each floor; **A** denotes the system matrix composed of structural mass, damping and stiffness ma-

trices; **B** represents the distributing matrices of the control forces; and **E** represents the distributing matrices for excitation.

The Equationn (3) is discretized in the time domain and excitation force is assumed to be constant within any time interval and can be written into a discrete-time form [17].

$$\mathbf{z}[k+1]=\mathbf{A}_d\mathbf{z}[k]+\mathbf{B}_d\mathbf{u}[k]+\mathbf{E}_d\mathbf{F}[k] \quad (5)$$

where $\mathbf{A}_d = e^{\mathbf{A}\Delta t}$ represents the discrete time system matrix with Δt as the time interval.

3. Numerical Study

The efficiency of double friction dampers installed in all the floors (Figure 4) of the benchmark building is investigated. The slip force of each friction damper is maintained as 150 kN. The performance of SAVDFDs using predictive control law installed in all the floors with complete state feedback is also investigated. In case of SAVFDs and SAVDFDs stiffness of bracing in each floor is maintained as 8.94e6 kN/m. Each semiactive friction damper is a bundle of 4 dampers. Wind tunnel tests [2] for the benchmark building model have been conducted at the University of Sydney and the results of across-wind data for a duration of 3600 s is provided for the analysis of the benchmark problem. However, in the present study the performance of dampers is studied for duration of 900 s. The time history and frequency content of across wind load at top floor of the building is shown in Figure 5. The response quantities and performance criteria of the benchmark building are studied.

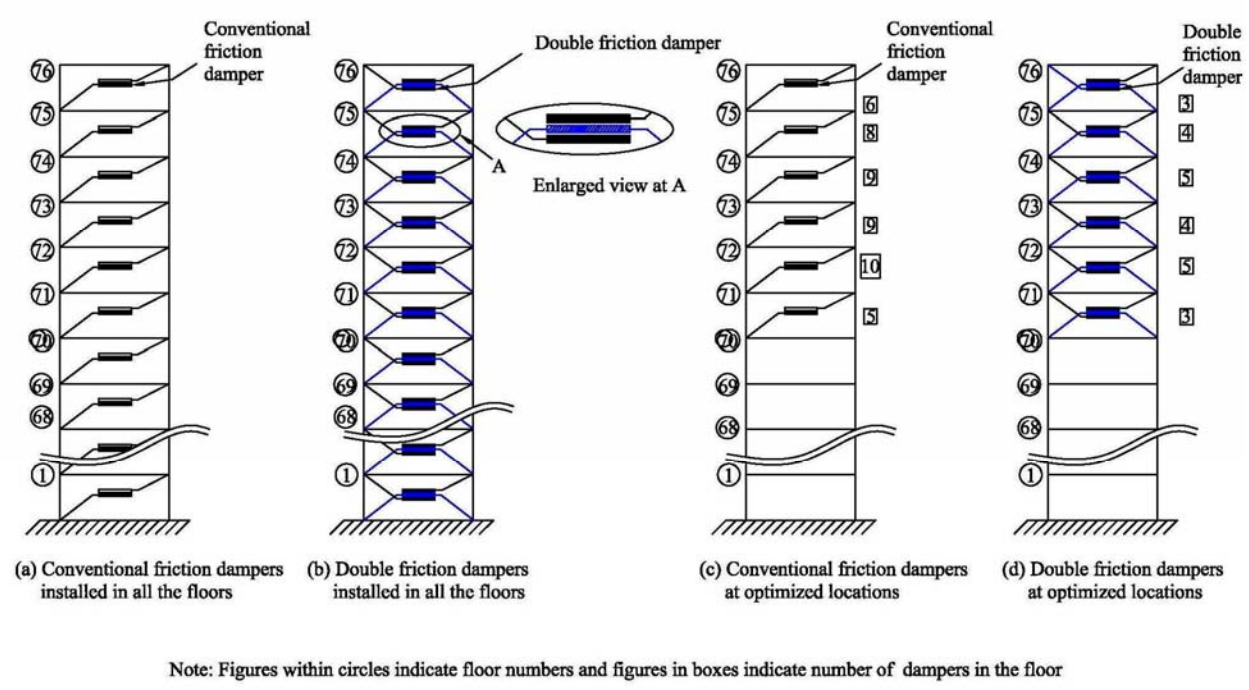

Figure 4. Various arrangements of friction dampers

The comparison of peak response quantities with the conventional friction dampers and double friction dampers installed at all the floors and at optimized locations is given in Table 2. Peak displacement quantities have reduced with the double friction dampers as compared to those with the conventional friction dampers. Peak acceleration quantities

have significantly reduced. The reductions in peak quantities are further improved at optimized locations. Thus, with the double friction dampers, the performance of the building has improved as compared to that with the conventional friction dampers. However, with the proposed double friction dampers, the improvement against acceleration is better than that against displacement.

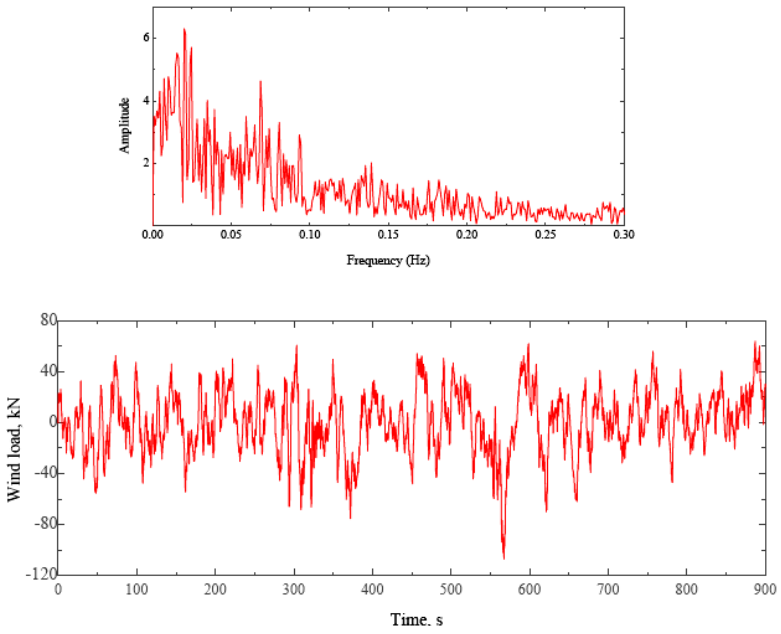

Figure 5. Comparison of frequency response and time variation of wind load at top floor of the benchmark building

Table 2. Peak response quantities of the benchmark building installed with friction dampers

Floor No	x_p(cm)					$\ddot{x}_p$(cm/s^2)				
	Number of Dampers									
	0	76†	76††	47‡	24‡‡	0	76†	76††	47‡	24‡‡
1	0.053	0.038	0.038	0.038	0.038	0.221	0.074	0.074	0.102	0.104
30	6.836	4.796	4.740	4.834	4.808	7.194	4.118	3.511	6.075	6.064
50	16.579	11.418	11.210	11.611	11.548	14.885	7.356	6.460	8.514	8.424
55	19.407	13.324	13.031	13.551	13.478	17.427	8.200	7.202	8.813	8.714
60	22.331	15.283	14.892	15.545	15.462	19.913	9.461	7.940	10.011	9.928
65	25.344	17.289	16.785	17.583	17.489	22.304	10.934	8.867	11.732	11.653
70	28.404	19.320	18.692	19.641	19.534	25.979	12.682	9.872	13.732	13.594
75	31.577	21.421	20.662	21.763	21.644	30.238	14.594	11.388	16.437	16.324
76	32.287	21.892	21.103	22.238	22.117	31.199	15.041	11.747	17.060	16.966

† Conventional friction dampers in all the floors
†† Double friction dampers in all the floors
‡ Conventional friction dampers, optimized
‡‡ Double friction dampers, optimized

From the results tabulated in Table 3, it is observed that the reductions in RMS quantities are considerable with the double friction dampers as compared to those with the conventional dampers. This is obvious as the number of sliding interfaces is doubled in the modified damper. With dampers at optimized locations the reductions are significant than those with the dampers in all the floors. Similar to peak accelerations, the reductions in RMS acceleration quantities are more as compared to those in RMS displacement quantities with the double friction dampers. From Table 4, it is seen that the performance criteria J_7 & J_8 which depend on peak acceleration quantities and J_1 & J_2 which depend on RMS acceleration quantities are reduced by a greater extent as compared to those which depend on peak displacement (J_9 & J_{10}) and RMS displacement quantities (J_3 & J_4).

Table 3. RMS response quantities of the benchmark building installed with friction dampers

Floor No	σ_x(cm)					$\sigma_{\ddot{x}}$(cm/s^2)				
	Number of Dampers									
	0	76†	76††	47‡	24‡‡	0	76†	76††	47‡	24‡‡
1	0.017	0.01	0.008	0.010	0.010	0.019	0.014	0.013	0.017	0.017
30	2.152	1.230	1.051	1.259	1.252	2.018	1.001	0.809	1.169	1.163
50	5.215	2.958	2.514	3.024	3.006	4.773	2.073	1.483	2.191	2.169
55	6.102	3.454	2.931	3.528	3.507	5.578	2.392	1.684	2.500	2.473
60	7.018	3.964	3.360	4.047	4.023	6.413	2.734	1.909	2.847	2.815
65	7.96	4.487	3.797	4.576	4.549	7.282	3.108	2.170	3.245	3.209
70	8.917	5.015	4.239	5.111	5.078	8.177	3.521	2.481	3.704	3.665
75	9.908	5.563	4.695	5.663	5.628	9.119	3.985	2.849	4.225	4.182
76	10.13	5.685	4.798	5.786	5.751	9.331	4.092	2.936	4.345	4.301

† Conventional friction dampers in all the floors
†† Double friction dampers in all the floors
‡ Conventional friction dampers, optimized
‡‡ Double friction dampers, optimized

Table 4. Performance criteria of the benchmark building installed with friction dampers

Criteria	Number of Dampers			
	76†	76††	47‡	24‡‡
J_1	0.437	0.312	0.463	0.458
J_2	0.431	0.304	0.452	0.447
J_3	0.561	0.473	0.571	0.567
J_4	0.564	0.477	0.575	0.571
J_7	0.483	0.377	0.544	0.540
J_8	0.484	0.400	0.530	0.525
J_9	0.678	0.653	0.689	0.685
J_{10}	0.682	0.663	0.694	0.690

† Conventional friction dampers in all the floors
†† Double friction dampers in all the floors
‡ Conventional friction dampers, optimized
‡‡ Double friction dampers, optimized

The peak quantities obtained with SAVFDs and SAVDFDs installed in all the floors and at their optimized locations are presented in Table 5. Similar to the trend shown by passive friction dampers peak quantities have considerably reduced with SAVDFDs as compared to those with SAVFDs. With dampers at optimized locations the enhancement in the performance is significantly high. The reductions in peak acceleration quantities are more than those in peak displacement quantities.

From Table 6, it can be seen that similar to the trend shown by passive friction dampers reductions in RMS quantities are seen with the proposed SAVDFDs. With dampers at optimized locations, the reductions are significantly high. Again with the proposed SAVD-FDs improvement in the performance against acceleration is better than that against displacement. And, from Table 7, performance criteria which depend on acceleration quantities (J_1, J_2, J_7 & $J_{8)}$ have reduced more than those (J_3,J_4,J_9 & J_{10}) which depend on displacement quantities.

Floor No	x_p(cm)					$\ddot{x}_p$(cm/s^2)				
	Number of Dampers									
	0	76†	76††	28‡	14‡‡	0	76†	76††	28‡	14‡‡
1	0.053	0.041	0.038	0.042	0.041	0.221	0.121	0.051	0.126	0.130
30	6.836	5.232	4.819	5.311	5.199	7.194	3.247	2.650	3.340	3.147
50	16.579	12.450	11.433	12.639	12.363	14.885	7.451	5.566	7.794	7.281
55	19.407	14.495	13.301	14.716	14.392	17.427	8.742	6.410	9.123	8.519
60	22.331	16.592	15.214	16.845	16.471	19.913	9.976	7.250	10.446	9.755
65	25.344	18.730	17.162	19.017	18.591	22.304	11.455	8.233	12.032	11.224
70	28.404	20.889	19.127	21.210	20.730	25.979	13.143	9.445	13.762	12.832
75	31.576	23.121	21.158	23.476	22.942	30.238	15.087	10.850	15.703	14.646
76	32.287	23.621	21.613	23.984	23.437	31.199	15.527	11.165	15.973	14.871

Table 5. Peak response quantities of the benchmark building installed with variable friction dampers

† SAVFDs in all the floors †† SAVDFDs in all the floors
‡ SAVFDs, optimized ‡‡ SAVDFDs, optimized

Comparisons of time histories as well as frequency responses of displacement and acceleration quantities of the 76th floor with the proposed double friction dampers and the conventional passive friction dampers installed in all the floors are shown in Figures 6 and 7 respectively. The displacement and acceleration quantities have considerably reduced with double friction dampers than those with conventional friction dampers. The comparisons of time histories as well as frequency responses of displacement and acceleration quantities of the 76th floor with SAVFDs and SAVDFDs installed in all the floors are made in Figures 8 and 9 respectively. Displacement and acceleration quantities of the 76th floor have considerably reduced with SAVDFDs as compared to those with SAVFDs. The amplitude of both displacement and acceleration frequency responses with both double friction dampers and SAVDFDs are reduced as compared to their conventional counter parts, corresponding to the frequency of 0.16 which is the fundamental frequency of the benchmark builing.

Table 6. RMS response quantities of the benchmark building installed with variable friction dampers

Floor No	σ_x(cm)					$\sigma_{\ddot{x}}$(cm/s^2)				
	Number of Dampers									
	0	76†	76††	28‡	14‡‡	0	76†	76††	28‡	14‡‡
1	0.017	0.010	0.009	0.011	0.010	0.019	0.009	0.007	0.009	0.009
30	2.153	1.339	1.173	1.377	1.330	2.018	0.995	0.740	1.038	0.972
50	5.216	3.228	2.821	3.321	3.206	4.773	2.347	1.741	2.474	2.317
55	6.103	3.772	3.293	3.880	3.745	5.578	2.741	2.032	2.892	2.707
60	7.019	4.331	3.778	4.456	4.300	6.414	3.150	2.335	3.326	3.113
65	7.961	4.906	4.276	5.048	4.870	7.282	3.577	2.650	3.775	3.533
70	8.918	5.488	4.780	5.647	5.447	8.177	4.016	2.975	4.235	3.963
75	9.909	6.090	5.301	6.267	6.044	9.119	4.479	3.318	4.731	4.430
76	10.131	6.225	5.418	6.405	6.177	9.332	4.583	3.394	4.800	4.488

† SAVFDs in all the floors
‡ SAVFDs, optimized
†† SAVDFDs in all the floors
‡‡ SAVDFDs, optimized

Table 7. Performance criteria of the benchmark building with variable friction dampers

Criteria	Number of Dampers			
	76†	76††	28‡	14‡‡
J_1	0.491	0.364	0.518	0.485
J_2	0.491	0.364	0.519	0.485
J_3	0.614	0.535	0.632	0.610
J_4	0.616	0.537	0.634	0.612
J_7	0.499	0.359	0.519	0.484
J_8	0.504	0.366	0.527	0.492
J_9	0.731	0.669	0.743	0.726
J_{10}	0.740	0.678	0.751	0.734

† SAVFDs in all the floors
†† SAVDFDs in all the floors
‡ SAVFDs, optimized
‡‡ SAVDFDs, optimized

With both the modified dampers reductions in accelerations is better than the displacements. Figure 10 shows the hysteresis loops of conventional friction damper and double friction damper at the 76th floor for different arrangements of dampers. For both the arrangements i.e. when dampers in all floors and at optimized locations the energy dissipated by the double friction damper is significantly higher than the conventional friction damper. Same observations can be made with the hysteresis loops of SAVFD and SAVDFD at 76th floor shown in Figure 11.

Thus, it is evident from the above observations that both the proposed dampers (double friction damper and SAVDFD) give better performance against displacement as well as acceleration as compared to their conventional counterparts. In both the proposed dampers, the improvement in the performance against acceleration is better than that against displacement.

3.1 Optimization of Location of Dampers

After studying the performance of the proposed dampers in all the floors, optimization of location and number of dampers is carried. Shukla and Datta (1999) [20] studied the optimal use of visco-elastic dampers (VEDs) in

the control of seismic response of multi-storey building frames using optimally placed VEDs. There can be various controllability indices depending upon the response quantities to be controlled. Here the controllability index is considered as

$$\chi(L) = \max \frac{\sigma_x(L)}{h(L)} \tag{6}$$

where $\chi(L)$ and $\sigma_x(L)$ are location index and RMS value of inter-storey drift at the L^{th} storey, respectively; and $h(L)$ is the L^{th} storey height. Thus, the L^{th} storey is the optimal location of a VED if $\chi(L)$ is maximum.

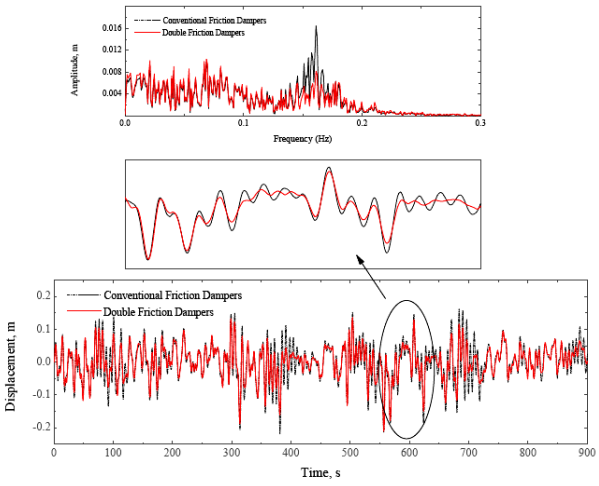

Figure 6. Comparison of frequency response and time variation of displacement of top floor with friction dampers installed in all the floors

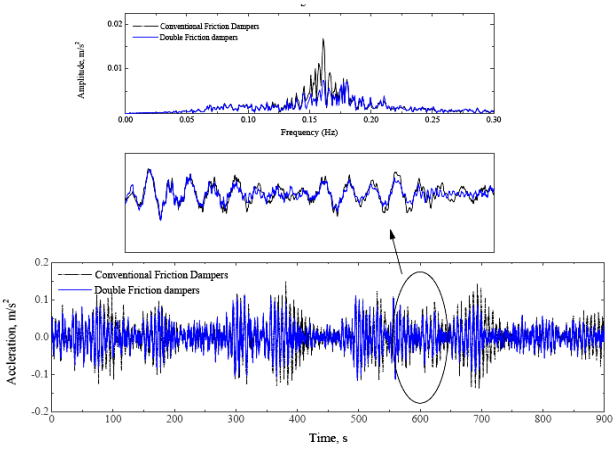

Figure 7. Comparison of frequency response and time variation of acceleration of top floor with friction dampers installed in all the floors

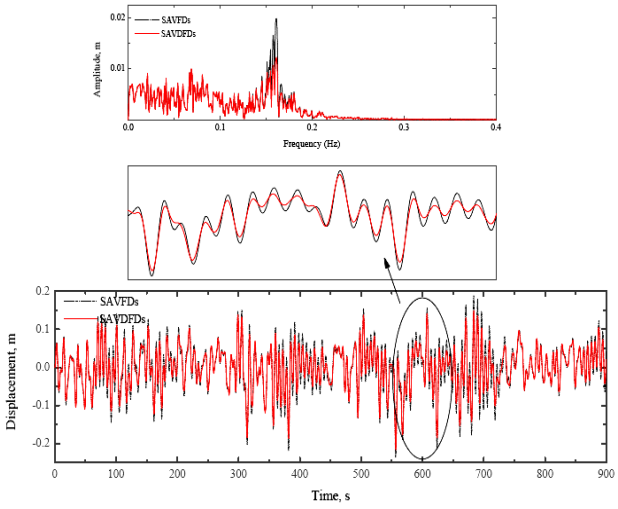

Figure 8. Comparison of frequency response and time variation of displacement of top floor with semi ative friction dampers installed in all the floors

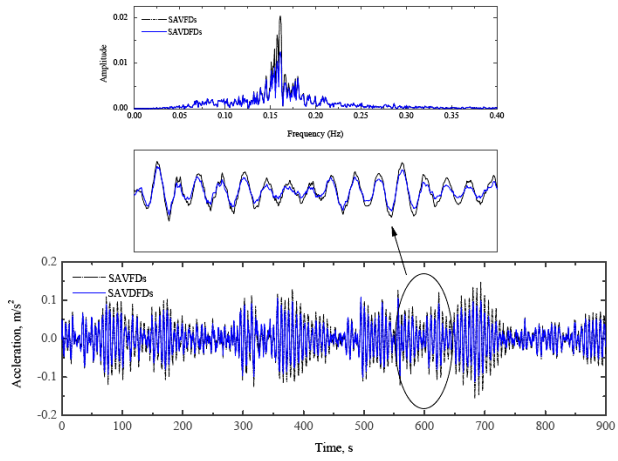

Figure 9. Comparison of frequency response and time variation of acceleration of top floor with semi active friction dampers installed in all the floors

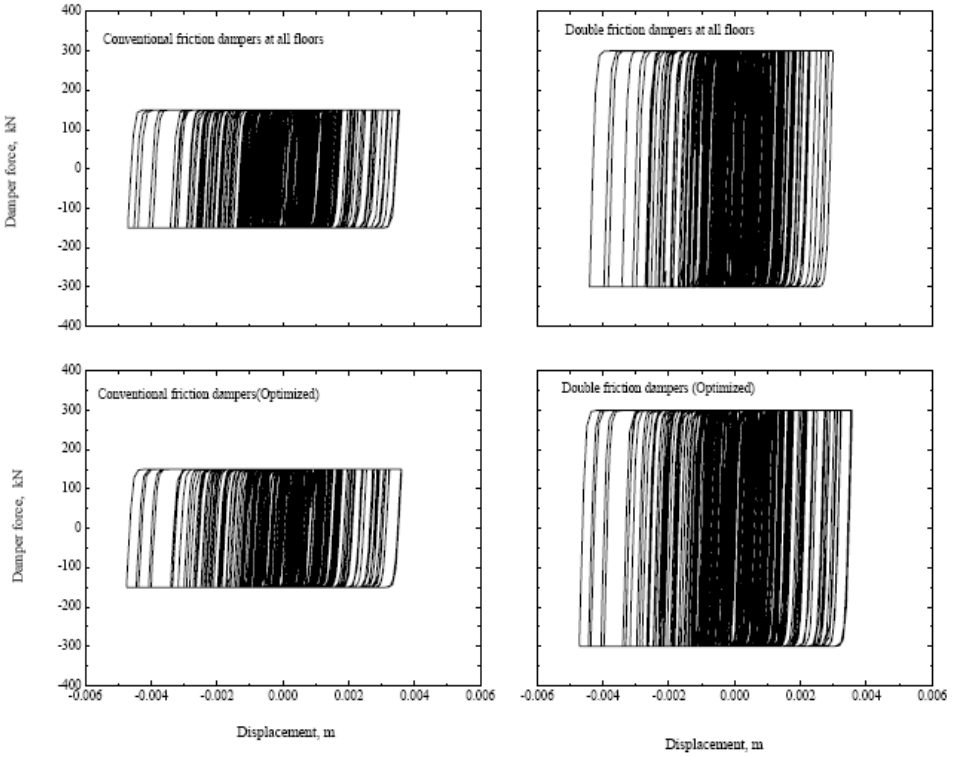

Figure 10. Hysteretic loops for friction damper at the top floor

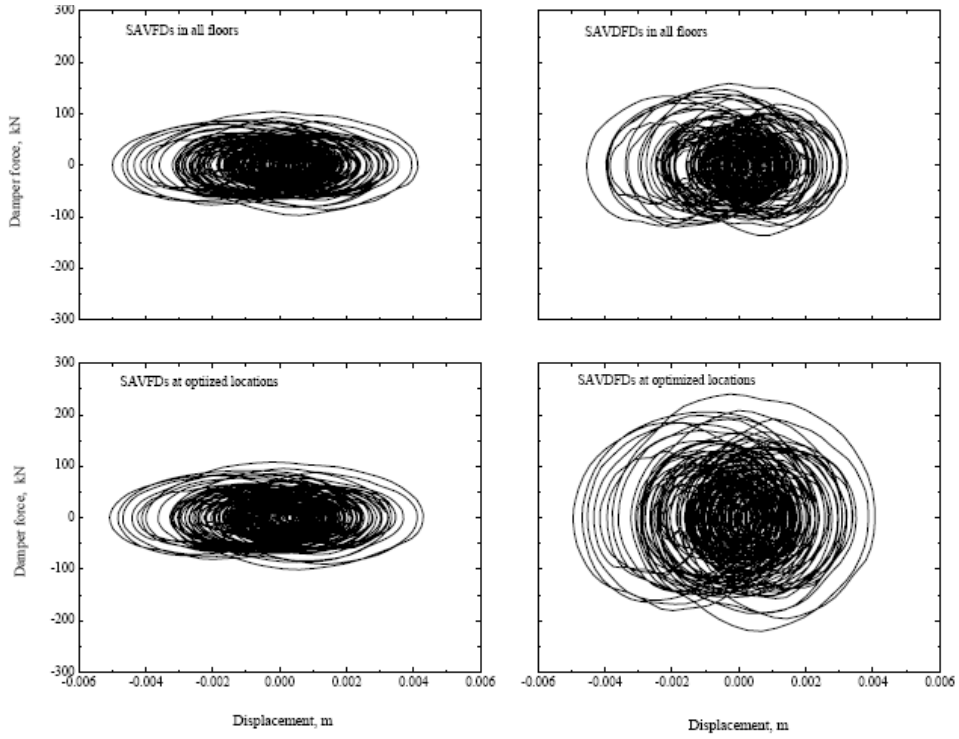

Figure 11. Hysteretic loops for semi-active friction damper at the top floor

Each damper is successively installed in the storey where the inter-storey drift is maximum. This is done with a view that a damper is optimally located if it is placed in the storey in which the displacement (or relative displacement) of the uncontrolled (or modified) structure is largest. This procedure is repeated until the required level of performance is achieved.

Optimization of location of double friction dampers and conventional friction dampers is carried out till the performance criteria are comparable to those obtained with the conventional friction dampers installed in all the floors. From Table 4, it is seen that at optimized locations, only 24 double friction dampers are sufficient to achieve the performance criteria comparable to those obtained with the conventional friction dampers installed in all the floors, whereas, 47 conventional friction dampers are required to achieve the same performance criteria.

From Figures 12 and 13, it is seen that at the optimized locations, 24 double friction dampers give displacement and acceleration values comparable to those obtained with 47 conventional friction dampers. Similar results are obtained with the SAVDFDs also (Figures 14 and 15). This achievement of similar performance with only half the number of both the proposed dampers is confirmed in the respective frequency responses. Thus, at the optimized locations, both the proposed dampers give 50% improved performance as compared to their conventional counterparts. The optimized location and number of friction dampers is shown in Figure 4. The optimized locations of friction dampers (both conventional and double friction dampers) are between 71 to 76^{th} floors. And, the optimized location of all the semi-active variable friction dampers (both SAVFDs and SAVDFDs) is at 76^{th} floor. Thus, the performance of the benchmark building is significantly enhanced with both the proposed dampers at their optimized locations.

3.2 Parametric Study

A parametric study is carried out with both conventional friction dampers (47 number) and double friction dampers (24 number) installed at their optimized locations (as explained in section 3.1), by varying slip force in the range of 150 to 2000 kN. Then plots of various performance criteria against slip force are shown in Figures 16 and 17. It is observed at optimized locations the number of double friction dampers is half of the conventional friction dampers to achieve the same values of criteria at every slip force. The values of J_1 and J_2 initially decrease attain a least value and then increase with the increase in slip force. Thus, there is an optimum value of slip force for the performance criteria J_1 and J_2. The optimum value of slip force for J_1 is 825 kN and that for J_2 is 725 kN. Similar behaviour is observed for the performance criteria J_7 and J_8. The optimum slip force for J_7 and J_8 is 1150 kN. For J_3, J_4, J_9 and J_{10} there is no optimum value of slip force as such. However, it is seen that the larger the value of slip forces the smaller the values of J_3, J_4, J_9 and J_{10}.

4. Conclusions

Numerical study of wind excited benchmark building with modified friction dampers (double friction damper and SAVDFDs) is carried out under the deterministic wind load. The comparison of the response quantities/ performance criteria is made with those obtained with their conventional counterparts to verify the effect of the modified dampers.

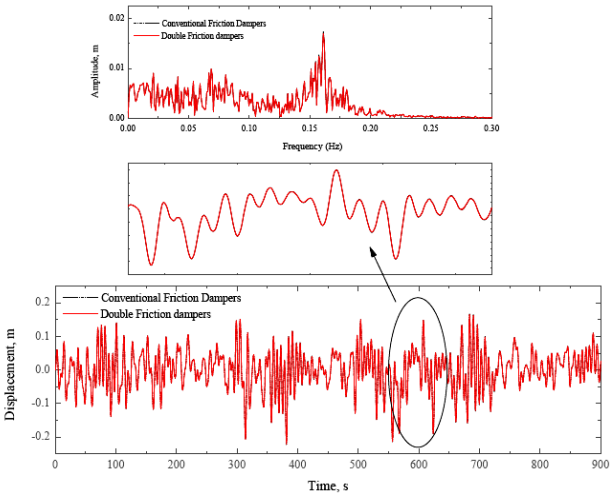

Figure 12. Comparison of frequency response and time variation of displacement of top floor with friction dampers installed at optimized locations

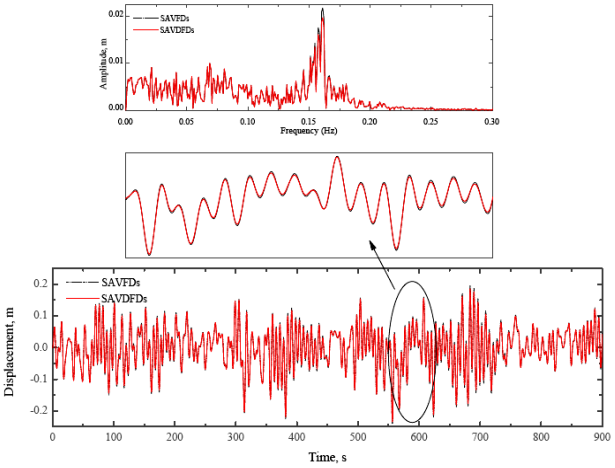

Figure 14. Comparison of frequency response and time variation of displacement of top floor with semi active friction dampers installed at optimized locations

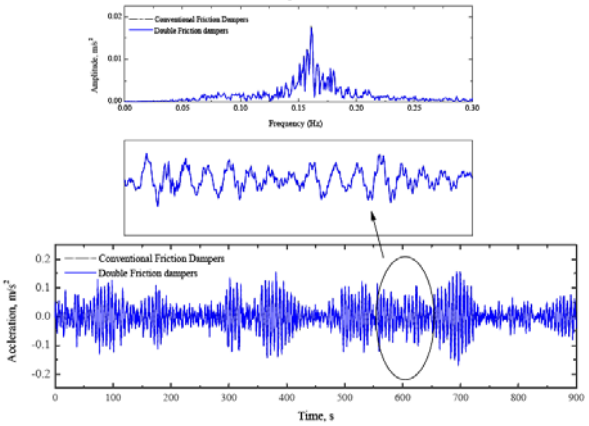

Figure 13. Comparison of frequency response and time variation of acceleration of top floor with friction dampers installed at optimized locations

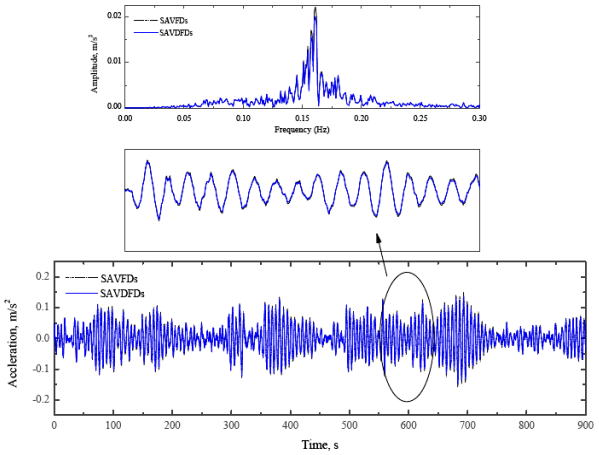

Figure 15. Comparison of frequency response and time variation of acceleration of top floor with semi active friction dampers installed at optimized locations

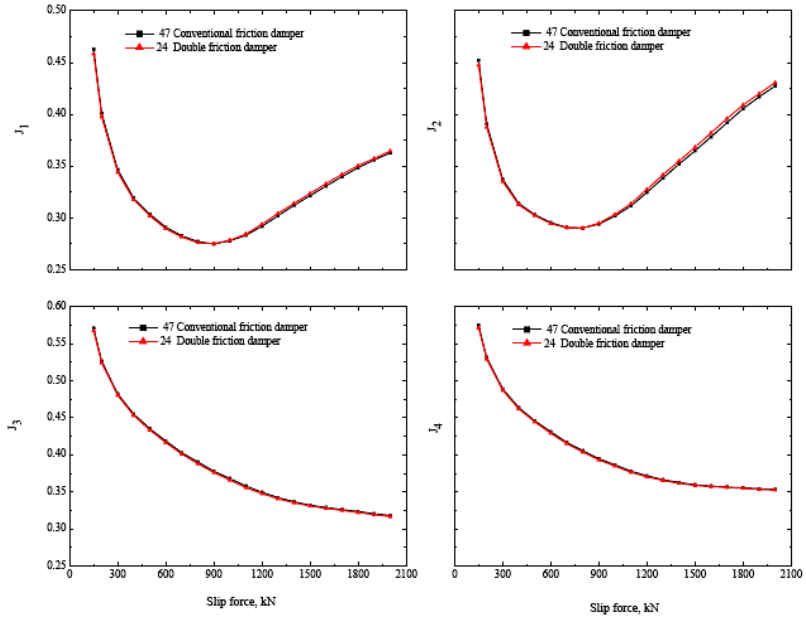

Figure 16. Variation of performance criteria (J_1-J_4) with slip force for the optimized location of friction dampers

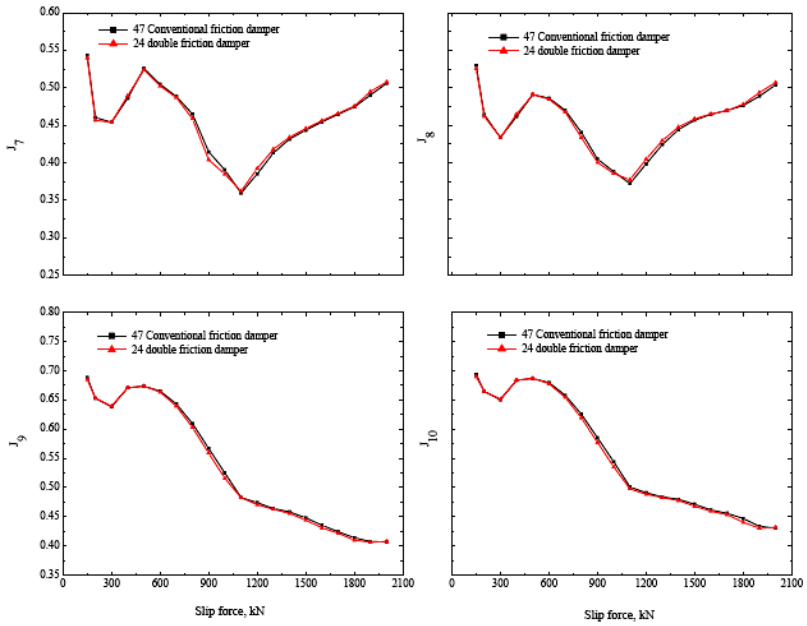

Figure 17. Variation of performance criteria (J_7-J_{10}) with slip force for the optimized location of friction dampers

Optimization of location of both conventional and modified dampers is also carried out and the results are compared. Additionally a parametric study is carried out to critically examine the performance of the building installed with passive friction dampers (both conventional and double friction damper) at their optimized locations. From the trends of the numerical results of the present study, the following conclusions may be drawn:

1. Both the proposed dampers (double friction damper and SAVDFD) give better performance against displacement as well as acceleration as compared to passive friction damper and SAVFD respectively. In both the proposed dampers, the improvement in the performance against acceleration is better than that against displacement.
2. At optimized locations both the modified dampers give significant enhancement in the performance of the benchmark building.
3. The optimized location of conventional and double friction dampers is between 71 to 76th floors.
4. The optimized location of all the SAVFDs and SAVDFDs is at 76th floor.
5. There exist optimum slip force both for conventional friction dampers and double friction dampers at their optimized locations for the performance criteria J_1, J_2, J_7 and J_8.
6. The larger the value of slip force the smaller the values of performance criteria J_3, J_4, J_9 and J_{10}.

Notation

Λ	Matrix of zeros and ones of order (n× r)
$\mathbf{A}$	System matrix
A	on-dimensional parameter of hysteretic loop
$\mathbf{A}_d$	screte-time system matrix
B	System matrix
$\mathbf{B}_d$	Coefficient matrices
C	matrix
$\mathbf{D}$	System matrix
E	Distributing matrices for excitation
$\mathbf{E}_d$	Coefficient matrices
f_{di}	Damper force of i^{th} damper
f_{si}	Slip force of i^{th} friction damper
Z_i	Non-dimensional hysteretic component i^{th} damper
F[k]	of wind load at k^{th} time step
$\mathbf{G}_u$	Augmented coefficient matrices
$\mathbf{G}_w$	Augmented coefficient matrices
$\mathbf{G}_z$	Augmented coefficient matrices
h(L)	L^{th} storey height
$\mathbf{I}$	Identity matrix
J1-J12	Performance criteria
$\mathbf{K}_b$	Diagonal matrix of stiffness of bracing
K_{bi}	Stiffness of bracing of ith damper
K	Stiffness matrix
$\mathbf{M}$	Mass matrix
n	Degree of freedom
n	Non-dimensional parameter of hysteretic loop
$P_{\max}$	Peak control power
r	mber of dampers
R_f	Gain multiplier
T	Total time of integration
X	Floor displacement vector
x_i	Displacement of i^{th} floor
x_{pi}	Peak displacement of i^{th} floor
x_{pio}	Uncontrolled peak displacement of i^{th} floor
x_{pm}	Peak stroke of actuator
$\mathbf{u}[k]$	Friction force vector at k^{th} time step
$\tilde{\mathbf{u}}[k]$	Critical friction force vector at k^{th} time step
$\mathbf{y}[k]$	Vector of drifts between the stories to which the dampers are connected
$\mathbf{z}$	State space vector
$\chi(L)$	Controllability index
σ_p	RMS control power
$\sigma_x(L)$	RMS value of inter-storey drift of

	L^{th} storey
σ_{xm}	RMS actuator stroke
$\dot{x}_m$	Actuator velocity
x_p	Peak displacement
$\ddot{x}_p$	Peak acceleration
σ_x	RMS Displacement
$\sigma_{\ddot{x}}$	RMS Acceleration
Δt	Time interval
ζ	Damping ratio
β	Non-dimensional parameter of hysteretic loop
τ	Non-dimensional parameter of hysteretic loop
μ	Coefficient of friction
Ni[k]	Normal force of ith damper at kth time step

References

[1] Yang, J. N., Agrawal, A.K., Samali, B., and Wu, J. C. 2004. Benchmark problem for response control of wind-excited tall buildings. *Journal of Engineering Mechanics*, 130: 437-446.

[2] Samali, B., Kwok, K. C. S., Wood G. S., and Yang, J. N. 2004a. Wind tunnel tests for wind-excited benchmark building. *Journal of Engineering Mechanics*, 15, 5: 447- 450.

[3] Min, K-W., Kim, H-S., Lee S-H, Kim, H., and Ahn, S. K. 2005. Performance evaluation of tuned liquid column dampers for response control of a 76-storey benchmark building. *Engineering Structures*, 27, 7: 1101-1112.

[4] Samali, B., Mayol, E., Kwock, K. C. S., Mack, A., and Hitchcock, P. 2004b. Vibration Control of the Wind-Excited 76-Storey Benchmark Building by Liquid Column Vibration Absorbers. *Journal of Engineering Mechanics*, 131, 4: 478- 485.

[5] Kim, H. and Adeli, H. 2005. Wind- induced motion control of 76-storey benchmark building using the hybrid damper-TLCD system. *Journal of Structural Engineering*, 131, 12: 1794-1802.

[6] Varadarajan, N., and Nagarajaiah, S. 2004. Wind response control of building with variable stiffness tuned mass damper using empirical mode decomposition/Hilbert transform. *Journal of Engineering Mechanics*, 130, 4: 451-458.

[7] Patil, V. B., Jangid, R. S. 2009. Response of wind excited benchmark building installed with dampers. The Structural Design of Tall and Special Buildings, USA (Accepted for publication).

[8] Bhaskararao, A. V., and Jangid, R.S. 2006a. Seismic analysis of structures connected with friction dampers. *Engineering Structures*, 28, 5: 690-703.

[9] Bhaskararao AV., and Jangid, R. S. 2006b. Harmonic response of adjacent structures connected with a friction damper. *Journal of sound and vibration* , 292, 3-5: 710-725.

[10] Akbay, Z., and Aktan, H.M. 1995. Abating earthquake effects on building by active slip brace devices. *Shock and Vibration*, 12, 2: 133-142.

[11] Kannan S, Uras, H. M, Aktan, H. M. 1995. Active control of building seismic response by energy dissipation. Earthquake *Engineering and Structural Dynamics*, 26, 3: 747-759.

[12] Inaudi, J. A. 1997. Modulated homogeneous friction: a semi-active damping strategy. *Earthquake Engineering and Structural Dynamics*, 26, 3: 361-376.

[13] Sadek, F., Mohraz, B. 1998. Semi-active control algorithms for structures with variable dampers. Journal of Engineering Mechanics: 981-990.

[14] Xu, Y. L., Qu, W. L., and Chen, Z. H.

2001. Control of wind-excited truss tower using semi-active friction damper. *Journal of Structural Engineering*, 127, 8: 861-868.

[15] Lu, L.Y., and Chung, L. L. 2001. Modal control of seismic structure using augmented state matrix. *Earthquake Engineering and Structural Dynamics*, 30, 2,: 237-256.

[16] Lu, L. Y. 2004a. Semi-active modal control for seismic structures with variable friction dampers. *Engineering Structures*, 26, 4: 437-454.

[17] Lu, L. Y. 2004b. Predictive control of seismic structures with semi-active friction dampers. *Earthquake Engineering and Structural Dynamics*, 33, 5: 647-668.

[18] Lu, L. Y., Chung, L. L., and Lin, G. L. 2004. A general method for semi-active feedback control of variable friction dampers. *Journal of Intelligent Material Systems and Structures*, 15, 5: 393-412.

[19] Kori, J. G., and Jangid, R. S. 2008. Semi-active friction dampers for seismic control of structures. *Smart Structures and Systems*, 4, 4: 493-515.

[20] Shukla, A. K., and Datta, T. K. 1999. Optimal use of Viscoelastic dampers in building frames for seismic force. *Journal of Structural Engineering,* 125, 4: 401-409.

[21] Constantinou, M., Mokha, A., and Reinhorn, A. M. 1990. Teflon bearing in base isolation, Part II: modeling. *Journal of Structural Engineering*, 130: 455-74.